Nanofiber Organic Semiconductors: The Effects of Nanosize on the Electrical Charge Transport and Optical Properties of Bulk Polyanilines

F. Yakuphanoglu,[1,2] R. Mehrotra,[3] A. Gupta,[3] M. Muñoz[2]

[1]*Department of Physics, Faculty of Arts and Sciences, Fırat University, 23119 Elazig, Turkey*
[2]*Instituto de Física Aplicada, Consejo Superior de Investigaciones Científicas (CSIC), Serrano 144, 28006, Madrid, España*
[3]*Optical Radiation Standards, National Physical Laboratory, Dr. K. S. Krishnan Marg, New Delhi 110012, India*

Received 6 December 2007; accepted 1 April 2008
DOI 10.1002/app.28535
Published online 15 June 2009 in Wiley InterScience (www.interscience.wiley.com).

ABSTRACT: The electrical transport, optical, and microstructural properties of bulk polyaniline (PANI) and nano-PANIs were investigated. A field emission scanning electron microscopy (SEM) image of bulk PANI showed macroscopic and aggregated granular particles. A SEM image of the nanostructured PANI showed the formation of one-dimensional nano/microstructures. The formation of nanofibers was observed from the transmission electron microscopy image. The electrical conductivities of the bulk and nanostructured PANIs increased with increasing temperature, which indicated semiconductor behavior. The electrical conductivities of the bulk and nanostructured PANIs at room temperature were found to be 2.12 $\times 10^{-5}$ and 1.80 $\times 10^{-2}$ S/cm, respectively. The electrical conductivity of the nanostructured PANI was about 850 times higher than that of the bulk PANI. The obtained band gaps of the bulk and nanostructured PANIs were determined from diffuse reflectance measurements and were found to be 3.27 and 2.41 eV, respectively. The refractive index of the PANI samples changed from 1.3 to 1.61. The obtained results indicate that the electrical and optical properties of the PANI were inherently dependent on the nanostructure. © 2009 Wiley Periodicals, Inc. J Appl Polym Sci 114: 794–799, 2009

Key words: activation energy; charge transport

INTRODUCTION

Semiconductor polyanilines (PANIs) have attracted considerable attention in electronic devices because of their electrical and optical properties. Polymeric molecules usually have dimensions ranging from 5 to 10 nm and are expected to exhibit size-dependent properties.[1] The behavior of organic polymers in nanoscopic systems has been found to be significantly different from their behavior in bulk samples, not only because of their reduced dimension but also because of their changed morphology.[2] Spectral characteristics are evidence for their peculiar behaviors at nanodimensional levels.[3] The strong dependence of UV spectra on nanoparticle size has been frequently observed.[1,4] The electronic[5] and optical properties[5,6] of these polymers in nanodimensions have been found to be different from those of bulk polymers. A fundamental understanding of how size and morphological changes influence the physicochemical properties of PANI nanoparticles is of great technological interest.[7] PANIs seem to be suitable candidates for nanoelectronic applications because of their optical and electrical properties, such as refractive index, optical band gap, and dielectric constant. The main goals of this study included the analysis of the electrical, optical, and microstructural properties of PANI and a fundamental understanding of how size changes influenced the electrical and optical properties of PANI. The effects of nanosize on the electronic and optical properties were analyzed by measurements of optical and electrical conductivity.

EXPERIMENTAL

The preparation of bulk and nanostructured PANIs was described elsewhere.[7] To study the electrical conductivity, bulk PANI and nano-PANI samples were pressed at 10 t/cm^2 to form a circular disc. Electrical conductivity was measured as a function of temperature with an alternating polarity method to eliminate electrical polarization and triboelectric and piezoelectric effects with a Keithley 6517A

Correspondence to: F. Yakuphanoglu (fyhanoglu@firat.edu.tr or fyhan@hotmail.com).
Contract grant sponsor: Turkish Scientific and Technological Research Council of Turkey (TÜBITAK); contract grant number: 105T137.

electrometer (USA). The alternating-current (ac) conductivity and impedance measurements were performed on a Hioki 3532 LCR instrument. The diffuse reflectance measurements of the PANIs were measured with a Shimadzu UV-3600-VIS-NIR spectrophotometer with a integrating sphere attachment. Barrium sulfonate was used as reference to provide a nominal 100% reflectance measurement. Field emission scanning electron microscopy (SEM) and transmission electron microscopy (TEM) images of all of the samples were obtained with a LEO 440 digital scanning electron microscope (resolutions: 3.5 nm in SEI mode and 5.5 nm in BEI mode) and a Phillips Morgani 268 microscope at a magnification of 14,000×, a resolution of 688 × 516 × 16, and an exposure time of 100 ms, respectively.

RESULTS AND DISCUSSION

Microstructural properties of the bulk and nanostructured PANIs

Figure 1 shows the SEM photographs of the bulk and nanostructured PANIs.[7] The field emission SEM image of bulk PANI showed macroscopic and aggregated granular particles.[7] Figure 1 shows the formation of well-defined rice-grain-type nanofibers between 300 and 500 nm and their lengths in 10s of micrometers. The SEM images of nanostructured PANI showed the formation of one-dimensional nano/microstructures. The TEM images of the bulk PANI and nano-PANI are shown in Figure 2. The TEM micrograph indicated the formation of nanofibers, as shown in Figure 2(b). Figure 3 shows the XRD patterns of the bulk PANI and nano-PANI samples. The diffraction pattern of the bulk sample was significantly different from that of nano-PANI, and nano-PANI showed sharp and well-resolved peaks.[7]

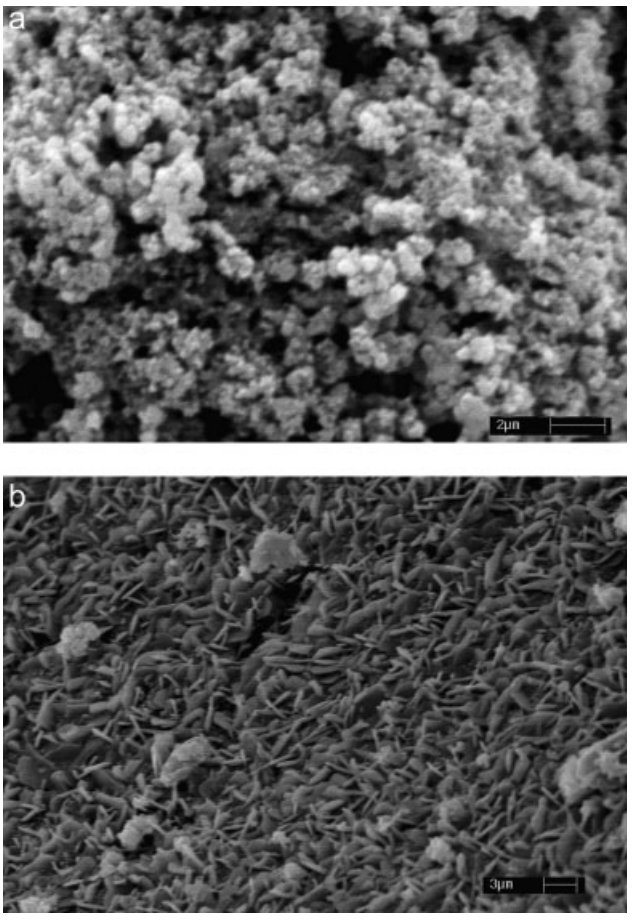

Figure 1 SEM micrographs of the (a) bulk and (b) nanostructured PANIs.

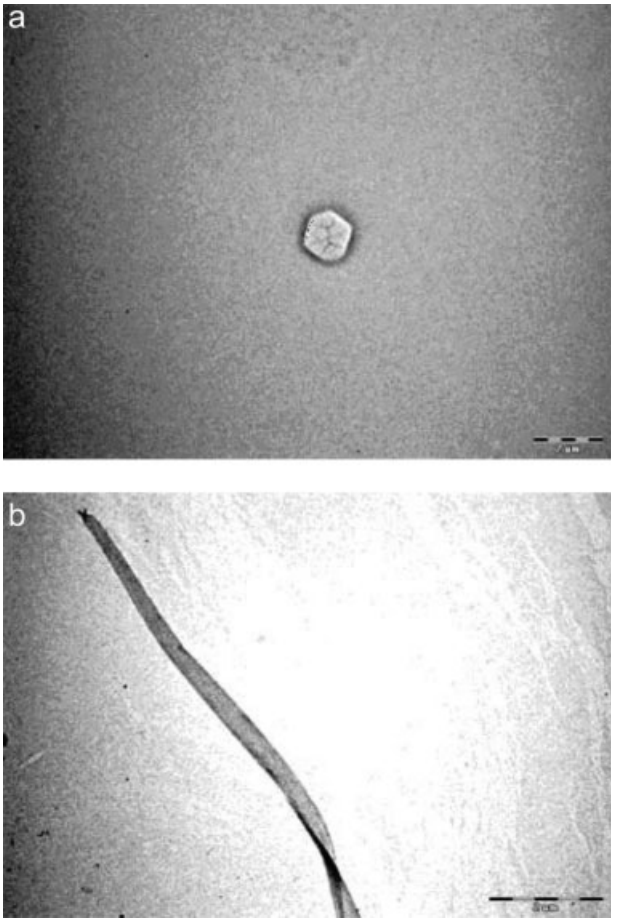

Figure 2 TEM micrographs of the (a) bulk and (b) nanostructured PANIs.

Direct-current (dc) conductivity properties of the bulk and nanostructured PANIs

The current (I)–voltage (V) characteristics of the bulk PANI and nano-PANI are shown in Figure 4. The I–V curves indicated ohmic behavior; that is, I changed linearly with V. Figure 5 shows the temperature dependence of the dc conductivity of the bulk and nanostructured PANIs. The plot of the

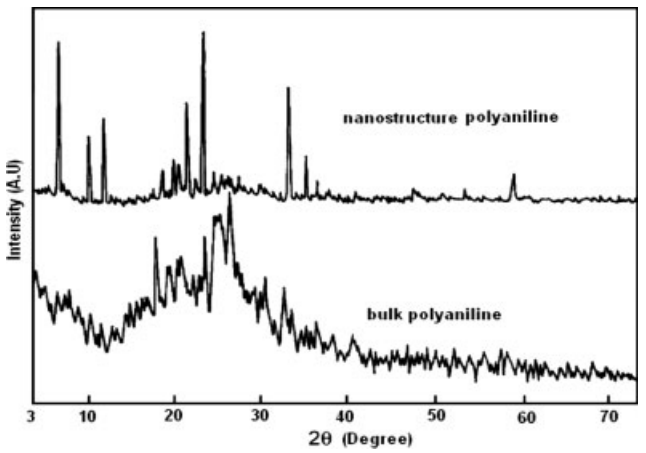

Figure 3 X-ray patterns of the bulk and nanostructured PANIs.

conductivity (σ) indicated linear regions that obeyed the following well-known relation:

$$\sigma = \sigma_o \exp(-E/kT) \quad (1)$$

where σ_o is the pre-exponential factor, E is the activation energy, k is the Boltzmann constant, and T is the temperature. The activation energies of the conductivity regions of the bulk PANI were found to be 0.29 and 0.46 eV, whereas the activation energy for the linear region of the nanostructured PANI was found to be 0.55 eV. The electrical conductivity curve of the bulk PANI indicated two linear regions and a transition region, whereas the nanostructured PANI showed a linear region and two nonlinear regions. The linear regions indicated that the electrical conductivity in the PANI samples took place via a thermally activated process. The electrical conductivities of the bulk and nanostructured PANIs showed semiconductor behavior; that is, the conductivity increased with increasing temperature. The electrical conductivities of the bulk and nanostructured PANIs at room temperature (at 25°C) were found to be 2.12×10^{-5} and 1.80×10^{-2} S/cm, respectively. The electrical conductivity of the bulk PANI was lower than that of the nanostructured PANI. The high conductivity was attributed to the nanostructure in the PANI. The electrical conductivity of the PANI increased with nanostructure. The conductivity of the studied nanostructured PANI was in agreement with the conductivity of PANI/Fe_3O_4 nanowire pellets (10^{-1}–10^{-2} S/cm).[8] We determined that we could control the microstructure to adjust the conductivity of the PANI semiconductor. The room-temperature electrical conductivity of this as-formed sample was found to be 5.68 S/cm;[7] after about 3 months, the electrical conductivity (1.80×10^{-2} S/cm) decreased significantly. This suggested that the polymer underwent molecular changes over time. The electrical conductivity resulted from the conjugation with charge carrier traveling through the backbone of the polymer with sufficient V.[9] We determined that the conjugation in the polymer was enough to make an organic semiconductor if it was present in the main chain of the polymer.[10]

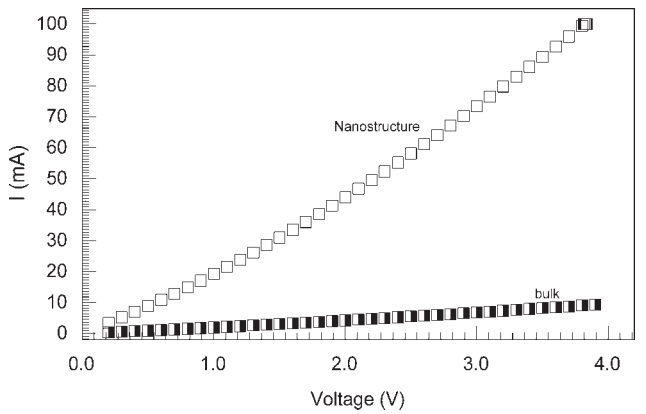

Figure 4 *I–V* characteristics of the bulk and nanostructured PANIs.

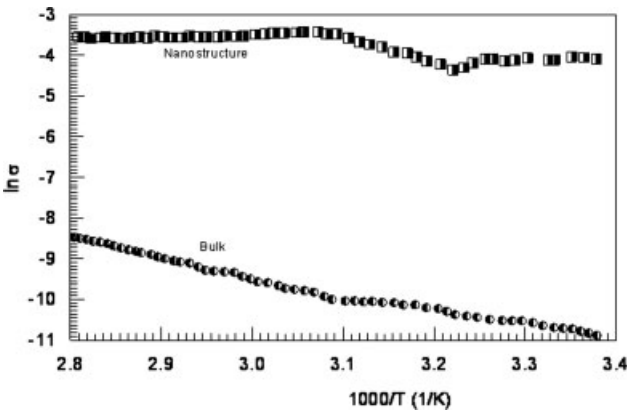

Figure 5 Temperature dependence on electrical conductivity of the bulk and nanostructured PANIs.

AC conductivity properties of the bulk and nanostructured PANIs

Figure 6(a,b) shows the plots of the ac conductivity of the bulk PANI and nano-PANI at different temperatures. The electrical conductivities of the bulk PANI and nano-PANI indicated two regions, which were frequency dependent and frequency independent. The first region corresponded to the dc conductivity, whereas the second region corresponded to the alternating conductivity. The ac electrical conductivity (σ_{ac}) of the samples was analyzed with the help of the following equation:[11,12]

$$\sigma_{ac}(\omega) = \sigma_{dc} + Af^s \quad (2)$$

where f is the angular frequency, σ_{dc} is the direct conductivity, A is a constant, and s is a constant that determines the type of conductivity mechanism. The ac electrical conductivities of the bulk PANI and nano-PANI increased with increasing temperature, and this increase in ac conductivity indicated that there may have been charge carriers, which were transported by hopping through the defect sites along the polymer chain.[13] The s values for the bulk PANI were calculated from the slope of the second conductivity region, and the s–T plot is shown in Figure 7. However, in the second region of nano-PANI, the conductivity increased up to 100 kHz with frequency and then decreased with increasing frequency. The obtained s values (0.0045–0.011) were lower than that of bulk PANI, and the s values did not exhibit any trend with temperature. The decrease in conductivity of the nano-PANI exhibited a metallic conductivity behavior because of the delocalized carriers present in metallic islands. The obtained s values for the bulk PANI decreased with increasing temperature (Fig. 7). This suggested that the correlated barrier hopping (CBH) model was

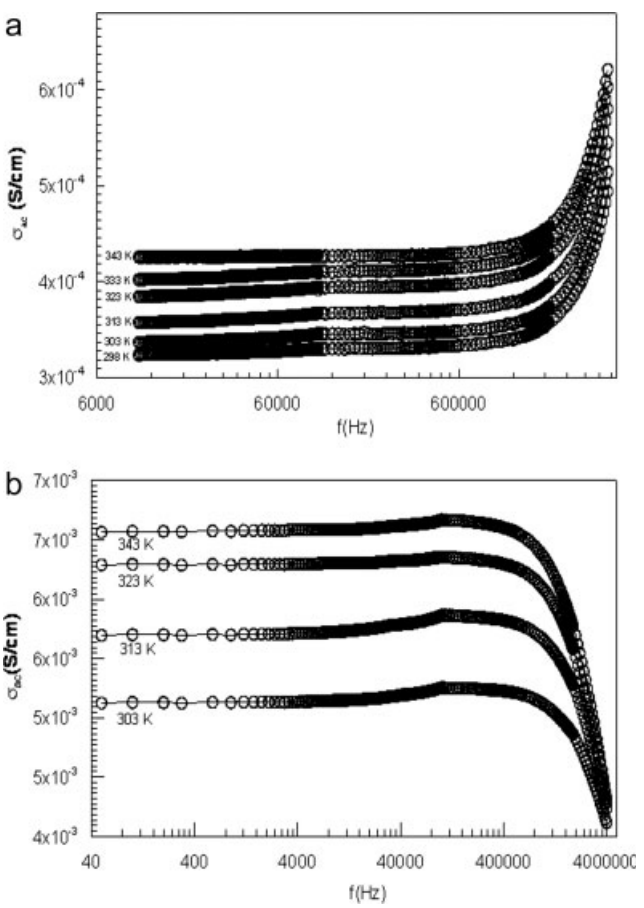

Figure 6 ac conductivity plots of the (a) bulk PANI and (b) nano-PANI.

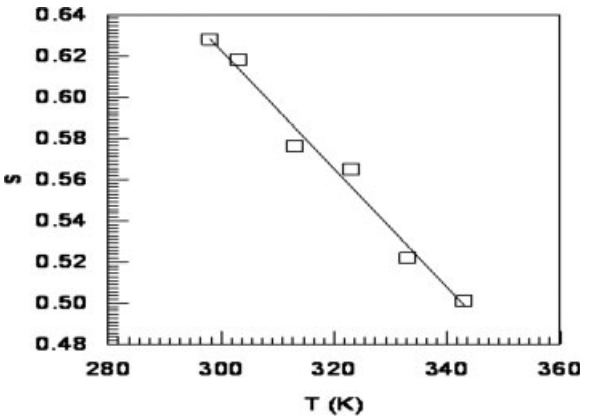

Figure 7 Plot of s versus T for the bulk PANI.

dominant in the sample. In the CBH model, the charge carrier hops between the sites over the potential barrier separating them.[14,15] The temperature dependence of s in the model is expressed as

$$s = 1 - \frac{6kT}{W_M - kT\ln(1/\omega\tau_o)} \quad (3)$$

where k is the Boltzmann constant, W_M is the binding energy of the carriers in localized states of the polymer, and τ_o is the characteristic relaxation time. The W_M value for the bulk PANI was calculated from the slope of the $1 - s$ versus T curve plotted with eq. (3) and was found to be 0.18 eV. Figure 8(a,b) shows the complex plane impedance plots for bulk PANI and nano-PANI at different temperatures. These plots indicated a single semicircle, which suggested that an equivalent circuit for the samples was represented by a resistance and a capacitor in parallel. Figure 8(b) shows the Cole–Cole plots for the nano-PANI, and the plots did not indicate the whole of the semicircle. For the bulk PANI, the diameter of the Cole–Cole curves decreased with increasing temperature. This suggested a temperature-dependent relaxation mechanism. We determined that in the investigated frequency range, the ac mechanism of the nano-PANI was different from that of the bulk PANI because of the higher electrical conductivity and nanostructure.

Optical properties of the bulk and nanostructured PANIs

The reflectance spectra of the bulk and nanostructured PANIs are shown in Figure 9(a). The reflectance spectrum of the bulk PANI showed a strong absorption band in the energy range 2–4.5 eV. The position of this band changed with nanostructure. The changes in the structure of the PANI gave new optical properties to the PANI. The optical band gap of the samples was obtained from the reflectance

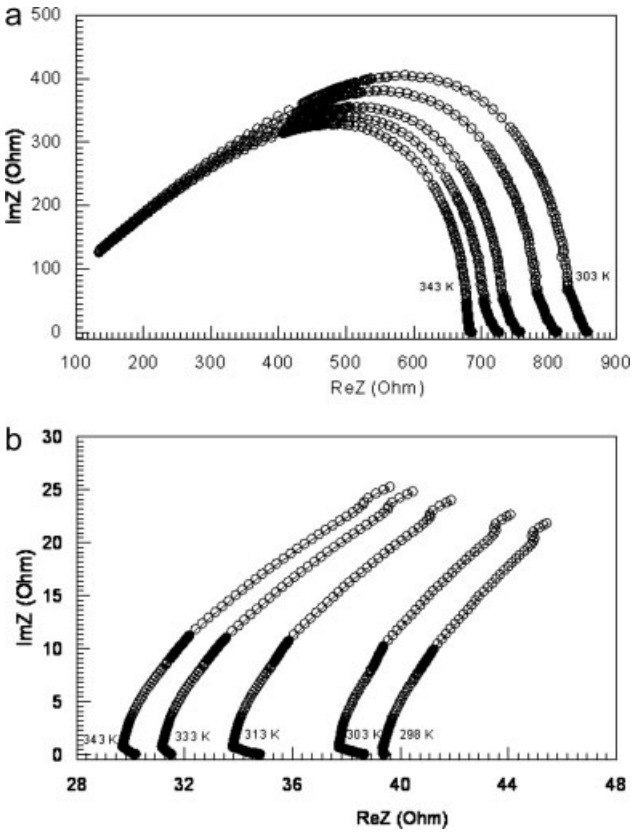

Figure 8 Plots of real ReZ and maginary ImZ parts of the impedance for the (a) bulk PANI and (b) nano-PANI.

spectra. For this, the absorbance was determined by application of the Munk–Kubelka function F:[16]

$$F(R_\infty) = \frac{(1-R_\infty)^2}{2R_\infty} = \frac{k}{m} \tag{4}$$

where R_∞ is the diffusive reflectance from infinitely layers, k is the absorption coefficient, and m is the scattering factor independent of the wavelength for particle sizes larger than the wavelength of light. We assumed that the well-known model of direct transitions were valid to determine optical band gap of the bulk PANI and nano-PANI. Thus, we plotted the curves of $(h\nu k/m)^2$ versus $E = h\nu$, h is the Planck constant, ν is the frequency. These are shown in Figure 9(b). The obtained band gaps of the bulk and nanostructured PANIs were determined from Figure 9(b) and were found to be 3.27 and 2.41 eV, respectively. The nanostructure of the PANI induced a decrease in the optical band gap of the bulk PANI. The optical band gap of the E_g bulk PANI was higher than that of PANI prepared by other methods (E_g = 3.04 eV[17] and E_g = 2.6 eV[18]) but was lower than that of another PANI (E_g = 3.65 eV),[19] whereas the optical band gap of the nano-PANI was lower than the previously mentioned PANIs. However, the optical band gaps of the both samples were higher

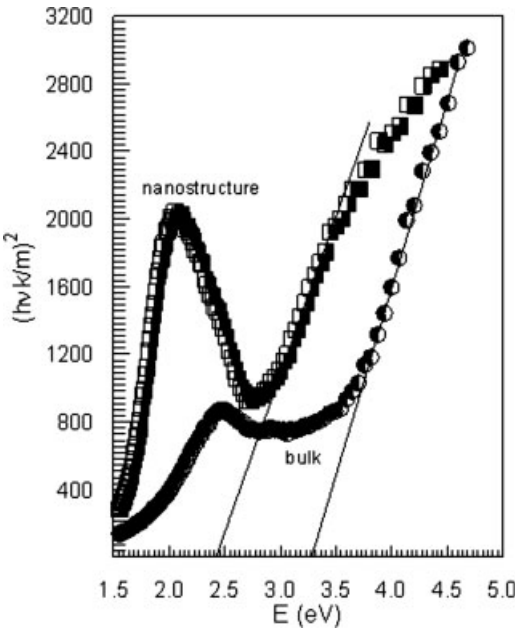

Figure 9 Curves of the reflectance and $(h\nu k/m)^2$ versus E of the bulk and nanostructured PANIs.

than that of another PANI (E_g = 1.68 eV).[20] This difference in the optical band gap was attributed to doping and nanostructure.

The refractive index dispersion properties of the bulk and nanostructured PANIs was analyzed by the following relation:[21]

$$R(\lambda) = \frac{[n(\lambda)-1]^2 + k(\lambda)^2}{[n(\lambda)+1]^2 + k(\lambda)^2} \tag{5}$$

where R is the reflectance, λ is the wavelength, n is the refractive index and k is the extinction coefficient. The refractive index of the samples was calculated by means of eq. (5). The spectral dependence of the refractive index is shown in Figure 10. The refractive index curve of the bulk PANI indicated a normal dispersion behavior between 350 and 500

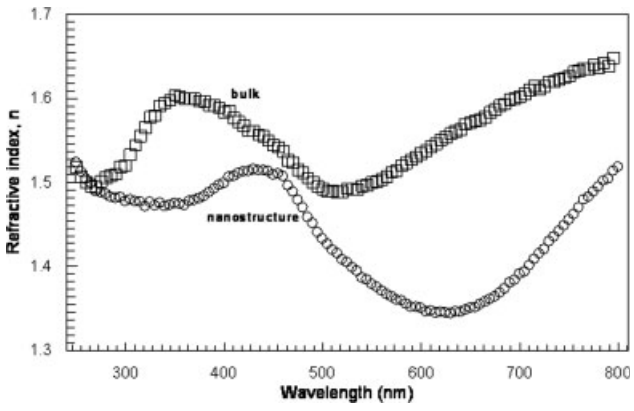

Figure 10 Refractive index spectrums of the bulk and nanostructured PANIs.

nm, whereas the nanostructured PANI indicated normal dispersion behavior in the range 450–620 nm. The refractive index dispersion of the PANI changed with nanostructure. This suggested that the refractive index of the PANI could be modified by nanostructure.

CONCLUSIONS

The electrical transport, optical, and microstructural properties of bulk PANI and nano-PANI were investigated. The electrical conductivity of the nano-PANI was higher than that of bulk PANI. The samples exhibited semiconductor behavior. The optical band gap of the bulk PANI decreased with nanostructure. The ac conductivity mechanisms of the samples took place via a CBH hopping conductivity mechanism. The nanostructure of the PANI modified the refractive index.

F. Yakuphanoglu thanks the Scientific and Technological Research Council of Turkey.

References

1. Chalmers, J. M.; Hannah, R. W.; Mayo, D. W. In Handbook of Vibrational Spectroscopy; Chalmers, J. M.; Griffithsin, P. R., Eds.; Wiley, 2001, vol. 3, p 1893.
2. Nealey, P. F.; de Pablo, J. J.; Ediger, M. D.; Cerrina, F. In Proceedings of the Conference on Nanoscale Science and Engineering, December, 2003.
3. Koeing, J. I. Spectroscopy of Polymers; American Chemical Society: Washington, DC, 1992.
4. Fu, H. B.; Yao, J. N. J Am Chem Soc 2001, 123, 1434.
5. Cho, M. S.; Park, S. Y.; Hwang, J. Y.; Choi, H. J. Mater Sci Eng C 2004, 24, 15.
6. Wu, T. M.; Lin, Y. W.; Liao, C. S. Carbon 2005, 43, 734.
7. Goel, S.; Gupta, A.; Singh, K. P.; Mehrotra, R.; Kandpal, H. C. Mater Sci Eng A 2007, 443, 71.
8. Long, Y.; Chen, Z.; Duvail, J. L.; Zhang, Z.; Wan, M. Phys B: Condens Matter 2005, 370, 121.
9. Yakuphanoglu, F.; Erol, I. Phys B: Condens Matter 2004, 352, 378.
10. Yakuphanoglu, F.; Basaran, E.; Şenkal, B. F.; Sezer, E. J Phys Chem B 2006, 110, 16908.
11. Hairetdinov, E. F.; Uvarov, N. F.; Patel, H. K.; Martin, W. Phys Rev B 1994, 50, 13259.
12. Mott, N. F.; Davis, E. A. Electronic Processes in Non-Crystalline Materials; Clarendon: Oxford, 1971; Chapters 2 and 7.
13. Jonscher, A. K. Thin Solid Films 1967, 1, 213.
14. Austin, I. G.; Mott, N. F. Adv Phys 1969, 18, 41.
15. Elliott, S. R. Adv Phys 1987, 2, 135.
16. Boldish, S. I.; White, W. B. Am Mineral 1998, 83, 865.
17. Mathai, C. J.; Saravanan, S.; Anantharaman, M. R.; Venkatachalam, S.; Jayalekshmi, S. J Phys D: Appl Phys 2002, 35, 2206.
18. Mukherjee, A. K.; Menon, R.; Pramana. J Phys 2002, 58, 233.
19. Sajeev, S.; Mathai, C. J.; Saravanan, S.; Ashokan, R. R.; Venkatachalam, S.; Anantharaman, M. R. Bull Mater Sci 2006, 29, 159.
20. Chithra Lekha, P.; Subramanian, E.; Pathinettam Padiyan, D. Sens Actuators B 2007, 122, 274.
21. Yakuphanoglu, F.; Liu, H.; Xu, J. J Phys Chem B 2007, 111, 7535.